Application of the generalised SAFT-VR approach for long-ranged square-well potentials to model the phase behaviour of real fluids

María Carolina dos Ramos[a,b,†], Hugh Docherty[b,†], Felipe J. Blas[a] and Amparo Galindo[b*]

[a] *Departamento de Física Aplicada, Facultad de Ciencias Experimentales, Universidad de Huelva, 21071 Huelva, Spain*

[b] *Department of Chemical Engineering, Imperial College London, South Kensington Campus, London SW7 2AZ, United Kingdom*

[†] *Current address: School of Chemical Engineering, Vanderbilt University, Nashville, TN 37235, US*

∗ *Corresponding author: a.galindo@imperial.ac.uk*

Abstract

In a recent generalisation of the SAFT-VR equation of state the method was extended so as to deal with wide square-well ranges, namely, $1.2 \leq \lambda \leq 3.0$ [B. H. Patel, H. Docherty, S. Varga, A. Galindo, and G. C. Maitland. *Mol. Phys.*, **103**(1), 129–139, 2005.]. In this work, this equation is used to revisit the adjustment of intermolecular model parameters, with special emphasis on substances where the upper boundary of the potential range ($\lambda = 1.8$) has been previously reported or may be expected on grounds of the polar nature of the molecules. For this purpose, we follow the work of Clark *et al.* [G. N. I. Clark, A. J. Haslam, A. Galindo, and G. Jackson. *Mol. Phys.*, **104**(22-24), 3561–3581, 2006] and study a relative least squares objective function and the percentage absolute average deviation (%AAD) to determine the intermolecular model parameters (m, λ, σ, ϵ/k_B, ϵ_{hb}/k_B and r_c) by comparison to experimental vapour-pressure and saturated liquid density data. In order to ensure in each case that the global minimum is identified, the dimensionality of the problem is reduced by discretising the parameter-space. Applying this method to the study of argon, nitrogen, benzene, carbon dioxide, carbon monoxide, n-alkanes, the refrigerant R1270, water, hydrogen chloride and hydrogen bromide, we find that the optimal models always present square-well ranges $\lambda < 1.8$, meaning that an upper bound value of $\lambda = 1.8$ (as set in the original approach) for the square-well range is sufficient to model real fluids. Accurate intermolecular potential models with ranges higher than 1.8 are also identified, but we find that these do not usually correspond to the global minimum of the objective function considered.

PACS numbers:

I. INTRODUCTION

The square-well (SW) intermolecular potential is one of the simplest models in which both repulsive and attractive interactions are included. It may be defined as

$$u^{SW}(r) = \begin{cases} \infty & \text{if } r < \sigma \\ -\epsilon & \text{if } \sigma \leq r \leq \lambda\sigma \\ 0 & \text{if } r > \lambda\sigma \end{cases} \tag{1}$$

where r is the intermolecular centre-to-centre distance, σ is the hard-core diameter, ϵ the depth of the well and λ its range.

The SW potential has been used as a model in many theoretical as well as numerical approaches, such as in the solutions of the Percus-Yevick, hypernetted chain and mean-spherical integral equations[1–3] and in the application of the high-temperature perturbation theory of Barker and Henderson[4]. In addition to this, it has been used in numerous simulation studies (see for example[5–9]), including the prediction of solid-solid[6] and glass-glass[10] transitions, reversible colloidal gelation[11] in systems of short-ranged SW particles, and in the study of confinement effects on the phase behaviour and structural properties of the SW fluid[9]. Further details may be found in the recent work of del Río *et al.*[12] which provides an excellent review, up to 2002, of key studies relating to the square-well fluid. Further to this, and in the context of this paper, the interested reader is directed to the work of Schöll-Paschinger *et al.*[13] who have studied the phase behaviour of square-well fluids of ranges $1.25 \leq \lambda \leq 3$ with a self-consistent Ornstein-Zernike approximation (SCOZA) and compared it to the perturbation approaches of Gil-Villegas *et al.*[14] for intermediate ranges and of Benavides and del Río[15] for long ranges. The SCOZA is found to be especially accurate for long-ranged ($\lambda > 1.5$) square-well fluids.

Of particular interest to us is the use of the SW fluid as a reference system in the development of equations of state for chain molecules such as those stemming from the thermodynamic perturbation theory (TPT) of Wertheim[16–21], which is commonly implemented in the form of the statistical associating fluid theory (SAFT)[22,23]. Since its development, many versions of SAFT have been proposed based on a wide variety of reference systems, such as the Hard-Sphere and Lennard-Jones fluids. An interesting development has been the acknowledgement of the importance of a variable potential range in the modelling of real fluids. In the SAFT-VR approach[24], intermolecular potentials of variable range are used to incorporate the non-conformal effects of fluids. We note that while in the modelling

of real fluids the most common reference system for this equation of state is a square-well fluid [25–33], the approach is general and, in the original work, was applied to the square-well, Yukawa, Sutherland and Mie potentials. However, in this work, we have chosen to use the square-well fluid as a reference system. Recently a Mie potential of variable repulsive range has been proposed to model phase coexistence and derivative properties[34,35] and, it has been shown that, the use of a variable repulsive range results in an excellent description of coexistence and derivative properties, yielding intermolecular potential parameters that follow physically-meaningful trends. These works provide further evidence of the importance of incorporating potentials of variable range.

In the SAFT-VR equation of state[24] the properties of the reference monomer fluid are obtained from a high-temperature perturbation expansion following Barker and Henderson[4,36,37] with a hard-sphere (HS) fluid as reference. Additionally, in order to obtain an analytical expression of the free energy, the mean attractive energy A_1 is written by mapping the radial distribution function of the reference fluid g^{HS} to the value of the function at contact using an effective packing fraction η_{eff} and the mean value theorem to solve the integral, such that

$$\frac{A_1}{NkT} = -\left(\frac{\epsilon}{kT}\right) 12\eta \int_1^\infty g^{\mathrm{HS}}(x;\eta)x^2 dx \approx -\left(\frac{\epsilon}{kT}\right) 4\eta g^{\mathrm{HS}}(1;\eta_{\mathrm{eff}}) \left(\lambda^3 - 1\right) \qquad (2)$$

where N is the number of molecules, k Boltzmann's constant, T the absolute temperature, η the packing fraction of the fluid and $x = r/\sigma$. Since it is possible to obtain the contact value for a hard-sphere fluid analytically using equations such as the Carnahan-Starling[38] equation, a numerical expression has effectively been replaced for an analytical one. Although this results in a loss of generality (as we discuss below the mapping of functions cannot be done in a general sense), analytical equations of state are more convenient in terms of speed of calculation and manipulation. In order to obtain the corresponding effective packing fraction in each case, the left hand-side of equation (2) is solved numerically for a range of η and λ values. In the original work, square-well potential values of λ between 1.2 and 1.8 were considered. Because of this, the SAFT-VR equation of state, employing a square-well potential to account for dispersive forces, is strictly only applicable for square-well fluids with a potential range of between 1.2 and 1.8.

The importance of the limits of the potential range for which the SAFT-VR equation of state may be confidently used becomes apparent when trying to obtain optimized parameters

for real fluids such as water or hydrogen fluoride, among others[39–41]. In these examples, the upper bound of $\lambda = 1.8$ is met on optimization, meaning that it is possible that an optimal model has not been obtained. One solution to this has been to use values $\lambda \geq 1.8$ for the potential range as it can be expected that the mapping will still provide accurate Helmholtz free energies when the bounds are only slightly exceeded. However, the relationship between η and η_{eff} quickly becomes more complex as $\lambda > 1.8$[42] and the original parametrization cannot be used. In a recent work a new mapping for the relationship between η and η_{eff} including values of $\lambda > 1.8$ (specifically for $1.2 \leq \lambda \leq 3.0$) has been presented[42]. Having tried a variety of expressions, a Padé approximant was proposed as it gives a good representation of both the simple (low λ) and complex (high λ) relationship of η_{eff} and η. The accuracy of the chosen expression was assessed by comparison with phase equilibrium data for a range of λ values obtained by computer simulation.

In this work, we investigate the applicability of the generalised SAFT-VR equation for square-well potentials[42] to model the phase behaviour of real substances. Specifically, we return to the study of substances in which the upper bound of $\lambda = 1.8$ has been previously reported as part of the optimized intermolecular parameter set, and of substances where their polar nature may suggest the need of longer intermolecular parameter ranges. In order to ensure that a global minima is achieved, we follow the work of Clark *et al.*[33] and study the objective function and the percentage of the absolute average deviation (%AAD) surfaces represented as two-dimensional contour plots where the axes correspond to two of the intermolecular parameters which are varied discretely so as to reduce the dimensionality of the problem.

The rest of the paper is organised as follows: details of the molecular models and theory are briefly reviewed in section II; the optimization procedure is presented in the section III; results are given in section IV; and discussion and conclusions are made in section V.

II. MOLECULAR MODEL AND THEORY

In the SAFT-VR approach, molecules are modelled as chains of m tangentially bonded spherical segments of hard-core diameter σ interacting via attractive potentials of variable range. In this work we consider square-well interactions. The square-well potential (Eq. 1) is characterized by a depth ϵ and a range λ. Hydrogen bonding and highly polar molecules

are treated by incorporating a number s of short-ranged attractive sites (association sites) of a given type that mediate the formation of aggregates. A model chain molecule is shown in Figure 1(a). The associating systems studied in the present work are water, hydrogen chloride and hydrogen bromide. The water molecule is modelled as spherical ($m = 1$) with four off-centre square-well attractive sites (two sites of type e represent the oxygen lone-pairs of electrons and two sites of type H represent the hydrogens), as shown in Figure 1(b). The hydrogen chloride and hydrogen bromide molecules are modelled as spherical ($m = 1$) with two off-centre square-well attractive sites (one site of type e represent the chloride and bromide lone-pairs of electrons and one site of type H represent the hydrogen), as shown in Figure 1(c) . The sites are placed at a distance r_d from the centre of the sphere, and have a cut-off range r_c. When two sites are closer than the cut-off distance r_c an attractive interaction of depth ϵ^{HB} is realised. Only H-e bonding is allowed (i.e., no H-H or e-e bonding).

The Helmholtz free energy corresponding to the models discussed is written in the SAFT-VR approach as a sum of four separate contributions

$$\frac{A}{NkT} = \frac{A^{IDEAL}}{NkT} + \frac{A^{MONO}}{NkT} + \frac{A^{CHAIN}}{NkT} + \frac{A^{ASSOC}}{NkT}. \tag{3}$$

The term A^{IDEAL} corresponds to the ideal free energy of the fluid, and A^{MONO}, A^{CHAIN} and A^{ASSOC} are the residual contributions to the free energy due to monomer-monomer interactions, chain formation and site-site intermolecular association (hydrogen bonding), respectively. Each of the contributions have been presented in detail in previous works[24,42] and so we do not provide further details here. Of particular interest to this work is the recent extension in which long-range square-well potentials are considered[42].

In the SAFT-VR approach the square-well monomer contribution is obtained from a Barker-Henderson[4,36,37] high-temperature perturbation expansion up to second order, i.e.,

$$\frac{A^{MONO}}{NkT} = \frac{A^{HS}}{NkT} + \frac{A_1}{NkT} + \frac{A_2}{NkT}, \tag{4}$$

where the hard-sphere reference free energy A^{HS} is given by the Carnahan-Starling expression[38] and, as mentioned in the introduction, the mean attractive energy A_1 can be expressed analytically by an appropriate mapping where the contact value of the radial distribution function at an effective density is used in place of the integral over the radial distribution

function (see equation (2)). A_2 is treated within the local compressibility approximation. For further details of the approach and of the specific expressions the reader is directed to the original papers[24,25,42].

In a previous work the mapping of densities used to obtain an analytical expression for the mean attractive energy (A_1) term was extended to treat square-well potentials of short ($\lambda \geq 1.2$) and long ($\lambda \leq 3$) range. A new parametrization was provided for this mapping, expressed as the Padé approximant

$$\eta_{\text{eff}} = \frac{c_1\eta + c_2\eta^2}{(1 + c_3\eta)^3}, \tag{5}$$

where the coefficients c_n are given by the matrix:

$$\begin{pmatrix} c_1 \\ c_2 \\ c_3 \end{pmatrix} = \begin{pmatrix} -3.16492 & 13.35007 & -14.80567 & 5.70286 \\ 43.00422 & -191.66232 & 273.89683 & -128.93337 \\ 65.04194 & -266.46273 & 361.04309 & -162.69963 \end{pmatrix} \begin{pmatrix} 1/\lambda \\ 1/\lambda^2 \\ 1/\lambda^3 \\ 1/\lambda^4 \end{pmatrix}. \tag{6}$$

As noted by Tan and colaborators [43] there was an error in Figure 1 of reference[42], in that the solid line was a guide to the eye and not the result of the theoretical calculation as provided by the parameterisation above. We note that the Helmholtz free energies obtained with the parameterisation presented are in very good agreement with the numerical values for the range of λ and η of interest. Although the more complex parameterisation of Tan *et al.*[43] provides better agreement for the mapping of densities, it is limited to $\lambda < 2.5$ and, in terms of the Helmholtz free energy, provides an essentially equivalent result to that of our work and is, as expected, not suitable for $\lambda > 2.5$ (see Figure 2). We also note in passing that the matrix presented by Tan *et al.*[43] appears to have the indexes ij in the wrong order. In Figures 3 and 4 the phase diagrams for square-well fluids of different ranges $\lambda > 2$ calculated using the SAFT-VR equation with the mapping of equations (5) and (6) and with that of Tan *et al.*[43] are compared with simulation data. The temperature-density and a Clausius-Clapeyron representation of the vapour pressure are given. Differences between the two parameterisations are seen more clearly in terms of the density. The main improvement seen with the more complex mapping of Tan *et al.*[43] is seen for $\lambda = 2.3$, in all other cases little or no difference is observed or, as in the case of $\lambda = 2$, our mapping turns out to be more accurate. In all, we feel that the simple mapping provided by equations (5) and (6) is perfectly suitable to describe the general phase behaviour of square-well fluids from short to long ranges ($1.2 \leq \lambda \leq 3$).

III. OPTIMISATION PROCEDURE

The equation of state discussed in the previous section has been applied to model the phase behaviour of a number of non-associating and associating compounds, with special emphasis on the effect of potential range in the optimization of intermolecular parameters. The intermolecular parameters (m, λ, σ, ϵ/k_B, ϵ^{HB}/k_B and r_c) of the SAFT-VR approach that characterize the compounds of interest are usually determined by comparison of calculated and experimental vapour-pressure and saturated liquid density data by minimising a relative least-squares objective function

$$f_{\text{objective}} = \left[\omega_p \sum_{i=1}^{N_{\text{exp},p}} \left(\frac{P_i^{\text{calc}} - P_i^{\text{exp}}}{P_i^{\text{exp}}} \right)^2 + \omega_{\rho_{liq}} \sum_{j=1}^{N_{\text{exp},\rho_{liq}}} \left(\frac{\rho_{liq_j}^{\text{calc}} - \rho_{liq_j}^{\text{exp}}}{\rho_{liq_j}^{\text{exp}}} \right)^2 \right] \quad (7)$$

where $N_{\text{exp},p}$ is the number of experimental pressure points, $N_{\text{exp},\rho_{liq}}$ the number of experimental saturated liquid density points, P_i^{exp} and $\rho_{liq_j}^{\text{exp}}$ are the experimental values of the vapour pressure and saturated liquid density of each point, respectively, and P_i^{calc} and $\rho_{liq_j}^{\text{calc}}$ are the corresponding vapour pressures and saturated liquid densities calculated with the SAFT -VR approach for a given intermolecular parameter set at the same temperature. The weighting factors ω_p and $\omega_{\rho_{liq}}$ are fixed equal to 1. The range of temperatures of the experimental data sets considered span from the melting point up to the critical point. However, it is well known that the critical region cannot be described with analytical equations of state such as SAFT-VR (a method to extend the approach to incorporate an accurate description of the critical region has been presented by McCabe and Kiselev[44,45] but we do not consider it here). In order to obtain an optimization of the intermolecular parameters that gives a better description of the low and intermediate temperature regions, the range of experimental temperatures in our work is limited to up to 90% of the critical temperature of the each pure substance.

It is also useful in comparing with experimental data to calculate the percentage absolute average deviation (%AAD) which is given by

$$\%\text{AAD} = \frac{1}{N_{\text{exp},p}} \sum_{i=1}^{N_{\text{exp},p}} \left| \frac{P_i^{\text{calc}} - P_i^{\text{exp}}}{P_i^{\text{exp}}} \right| + \frac{1}{N_{\text{exp},\rho_{liq}}} \sum_{j=1}^{N_{\text{exp},\rho_{liq}}} \left| \frac{\rho_{liq_j}^{\text{calc}} - \rho_{liq_j}^{\text{exp}}}{\rho_{liq_j}^{\text{exp}}} \right|. \quad (8)$$

While we use the objective function of equation (7) to estimate the model parameters, we use the %AAD as a measure of the error of the calculation.

In multiparameter equations of state, such as SAFT-VR, it is difficult to determine an optimal set of intermolecular potential model parameters from local-search algorithms without resorting to global minimisation methods. A simple method that takes advantage of the speed of local methods but implements, to a degree, a global view of the objective function space as been presented recently[33]. The idea is to reduce the dimensionality of the problem by fixing the value of two of the parameters at discrete intervals that eventually encompass the entire parameter space. The reduction of the dimensionality provides faster convergence of each of the minimisation problems. The space is then analysed in two-dimensional contour plots, of the error or objective function, and areas that may contain the global minimum are identified. Each point of the two-dimensional grid is an evaluated point of the minimum value of the objective function, with a corresponding %AAD (see equations (7)-(8)), obtained with two parameters fixed (as corresponding to the axes of the grid) while all other parameters are optimized to the experimental vapour pressure and saturated liquid density data using a combined simplex and annealing method[46]. In particular, the potential range λ is used in this work as one of the fixed variables at each grid-point. Our aim is to ensure that a global minimum is identified, so as to determine if models with $\lambda > 1.8$ need to be considered in modelling the experimental phase behaviour of pure compounds. In some cases we have also carried out optimizations with m fixed, so as to be able to compare with models previously presented.

In the case of non associating molecules for each fixed λ, there remain three parameters to be determined. Therefore, three possible contour-plots can be studied: the chainlength (m) *versus* potential range (λ), the segment diameter (σ) *versus* potential range (λ) and energy parameter (ϵ/k_B) *versus* potential range (λ) (not considered here). Details of the grids considered in each case are given below:

- $m - \lambda$ plot:

  Values of $1.00 \leq m \leq 6.00$ for the chain length and values of $1.20 \leq \lambda \leq 3.00$ for the potential range are considered. The intervals for each variable used in the grid are $\Delta m = 0.05$ and $\Delta\lambda = 0.018$. The total number of evaluated points is 10201.

- $\sigma - \lambda$ plot:

  Values of 1.00 Å $\leq \sigma \leq$ 6.00 Å in intervals of $\Delta\sigma = 0.05$ Å and potential range values $1.20 \leq \lambda \leq 3.00$ in intervals of $\Delta\lambda = 0.018$ are considered. The total number of

evaluated points is 10201.

Given the global nature of the method, any of the surfaces discussed is expected to lead to the same optimal model. We have confirmed this for each of the substances studied.

In the case of associating molecules, the number and type of association sites need to be specified, and the site-site association energy (ϵ^{HB}/k_B), and the association cut-off length (r_c) are optimized by comparison to experimental data. There are hence a number of additional two-dimensional grids that may be constructed. Since the association interaction plays an important role in the thermodynamic properties of these compounds (and especially in water, which is of interest in this work), we construct the contour plots of the objective and %AAD surfaces for fixed λ and ϵ^{HB}/k_B. We have selected λ as the parameter to be controlled discretely as opposed to ϵ, which was used in the work of Clark *et al.*[33], as we are particularly interested in investigating models with long potential ranges. In the SAFT-VR approach the dipole of water is not incorporated explicitly, so that a longer square-well range may be expected. We treat values $1000\,\mathrm{K} \leq (\epsilon^{HB}/k_B) \leq 1600\,\mathrm{K}$ at intervals of $\Delta(\epsilon^{HB}/k_B) = 6\,\mathrm{K}$ and values $1.20 \leq \lambda \leq 3.00$ for the potential range in intervals of $\Delta\lambda = 0.018$. In total 10201 optimizations are carried out.

For clarity, in the figures presented in the following section only grid points with values of the objective function ($f_{\mathrm{objective}}$) between $[0-1]$ and values of the %AAD between [0-5]% are plotted. Values higher than these for both functions correspond to models that are deemed unsatisfactory, they provide no useful information and are represented as white regions in the plots. Once the interesting areas of the parameter space are determined, the grid minimum is identified. In a final step, all intermolecular parameters are optimized using the grid minimum as a starting point, and setting tight bounds for all parameter values.

IV. RESULTS

We have applied the method discussed in the previous section to determine optimal intermolecular model parameters for a range of substances. We have chosen argon as representative of the simplest non-polar spherical molecules, and four n-alkanes as representatives of non-polar chain-like molecules; these have been thoroughly studied with SAFT-like approaches, so they provide a good means of comparison. We consider also a number of quadrupolar molecules (nitrogen, benzene, carbon dioxide) which can be expected to find

corresponding molecular models of longer range, refrigerant R1270 (propene), and dipolar molecules such as carbon monoxide, hydrogen chloride and hydrogen bromide and water which also presents string hydrogen bonding interactions. Our aim is to assess if in modelling real substances there is a need to incorporate square-well potentials of very long range.

The optimal parameters for the substances studied are presented in Tables I and II together with values already presented in the literature, which are given for comparison. It is useful to recall that when comparing the values of intermolecular parameters and deviations with the current method and with the original SAFT-VR approach small differences are expected in all cases. Although some effort was placed in the development of the generalised version to maintain the mapping between η and η_{eff} as close as possible to the original SAFT-VR equation for $1.2 \leq \lambda \leq 1.8$, the two are not mathematically identical. The experimental data was obtained mostly from the Detherm® database.[47] In addition, all references that were used in the evaluation the objective function and the %AAD are given explicitly for each substance. In Figures 5-8 a sample of the contour plots of the objective function and %AAD obtained for benzene, carbon dioxide, *n*-butane and water are presented. In each case well-defined areas of minima are identified. It should be noted that only water has previously been treated with a global approach as carried out here.

A. Non-polar molecules

It is useful to treat first non-polar molecules, which provide a reference for the value of the square-well range related to real compounds. We first consider argon. This simple molecule is treated as spherical with $m = 1$, the remaining parameters (λ, σ and ϵ/k_B) are optimized as described above. A well-defined single minimum region is observed for $\lambda = [1.4 - 1.6]$ and $\sigma = [3 - 3.6]$ Å. The minimum of all evaluated points can be found at $\lambda = 1.5$ and $\sigma = 3.3$ Å. With the values of the parameters found at this evaluated point, we perform a final optimization considering only values that are inside of this region. The optimized parameters and the resulting %AAD are presented in Table I.

The homologous series of the *n*-alkanes is also of general interest given their importance as components of crude oil, as oligomers of polyethylene, and as ideal chain-like molecules with which to test molecular models and theories. In addition, mixtures of *n*-alkanes and polyethylene molecules exhibit a variety of interesting phase behaviours[53–55]. Here we revisit

the models and parameter sets for four of the smaller n-alkanes: ethane, propane, n-butane and n-octane. We minimise the objective function, studying an $m - \lambda$ grid and, for fixed values of m as used in the literature, we construct contour plots of the objective function and the %AAD in the $\sigma - \lambda$ plane. An example of the type of surface obtained for the n-alkanes is given in Figure 5 (n-butane is chosen as a characteristic molecule). While a relatively wide range of minima is obtained for optimizations with free m, a better defined region of minima is seen in the case of models with m fixed. The optimal parameter sets for the four n-alkanes considered are presented in Table I. Two key conclusions can be drawn from these calculations: we find that by fixing m the surface of the objective function is better behaved with less local minima, a second conclusion is that none of the optimal models presents a value of the square-well range λ greater than 1.8.

B. Quadrupolar molecules

Benzene is highly non-spherical and strongly quadrupolar due to the delocalisation of electrons in the aromatic ring and, as such, it may be expected that a larger value of λ will be necessary to account for the long range nature of these interactions. The $m - \lambda$ surfaces of the objective function and %AAD are shown in Figure 6. We note that while in both figures a region of possible interest extends to longer values of λ, a discrete region of lowest minima occurs around a grid minimum value located at $m = 2.750$ and $\lambda = 1.722$. Further refinement of this region using tight bounds around the grid minimum results in the optimal set of intermolecular model parameters presented in Table I which are consistent with recently published parameters for the same system[48]. Small differences can be attributed to the different mappings in the generalised SAFT-VR equation of this work and the original one used in reference[48]. A main conclusion of our calculations is that even for the case of a strongly quadrupolar molecule such as benzene, the optimal set of intermolecular parameters identified corresponds to one with $\lambda < 1.8$.

Another quadrupolar molecule of interest is carbon dioxide (CO_2), which has become a useful replacement for organic solvents and is particulary important in supercritical extraction applications due to its relatively accessible critical point. In previous works a model of two tangentially bonded segments, i.e., $m = 2$ has been presented and used to study the phase behaviour of mixtures containing CO_2 very successfully[49–52]. Here, we carry out

minimisations of the objective function in an $m - \lambda$ space, and also consider models with $m = 2$ fixed, where we study the $\sigma - \lambda$ space. In Figure 7 the objective function and %AAD in each of the spaces are presented. As can be seen in the top figures (a) and (b), in the case where m is an optimizable parameter, an almost linear region of lowest minima is observed, running from $m = 1$, $\lambda = 1.3$ to approximately $m = 4.5$ and $\lambda = 2.2$. However, further resolution leads to a grid minimum value of the objective function at $m = 3.050$ and $\lambda = 1.7580$. The final set of parameters obtained in a minimisation with this starting point and tight bounds is presented in Table I. The optimizations carried out with fixed $m = 2$ (Figures 6(c) and 6(d)) clearly present a better behaved surface with a smaller region of equivalent parameter sets. The minimum of the grid in this case is found for $\lambda = 1.542$ and $\sigma = 2.750$ Å; the optimal set of parameters is presented in Table I. It is also interesting to note the relation between σ, ϵ and λ in the integrated mean-field parameter $\alpha = 2\pi\sigma^3\epsilon(\lambda^3 - 1)$, so that combinations of these parameters leading to the same value of α result in very similar thermodynamic properties. Note however that small differences can be expected in modelling chain molecules as the contribution to the free energy due to the formation of a chain is explicitly dependent on λ.

For comparison, the values of the CO_2 molecular parameters obtained in previous works[49,50] are given in Table I with corresponding values of %AAD obtained with the same experimental data, but using the original SAFT-VR approach. As can be seen, the parameters of the two approaches (for a fixed $m = 2$) are very close and the differences in the value of %AAD small. These results are entirely justified based on the fact that the mapping presented in the generalised SAFT-VR equation[42] was developed in such a way that for $\lambda < 1.8$ the parameterisation of the effective packing fraction can be compared to that of the original SAFT-VR, and that, as discussed earlier, models developed with a priori fixed values of m lead to objective functions with less local minima, so that in most cases the global minimum can be identified easily with local search methods.

We have also developed a model for nitrogen. As for CO_2, we consider two grids: one in which the number of segments m is optimized, and another in which m is fixed. In the first case a grid in the space $m - \lambda$ is constructed, and multiple local minima of similar depth are observed, which highlights the importance of considering global methods. A minimum is identified at $m = 1.4$ and $\lambda = 1.55$ (with corresponding values of $\sigma = 3.1488$ Å and $\epsilon/k_B = 84.294$ K). Using this as the starting point for a final optimization with

tight bounds, the optimal model is found (see Table I). In order to compare with optimal parameters previously presented by Haslam *et al.*[32], in the second grid the value of m is fixed to 1.3 and a $\sigma - \lambda$ surface is calculated. We observe that, as in the case of CO_2, setting the value of m to a fixed value greatly reduces the number of local minima on the surface of the objective function. The optimal model found is presented in Table I. The values of the intermolecular parameters for nitrogen obtained by Haslam *et al.*[32] are included in the table for comparison. As can be seen from Table I, the model obtained in this work is entirely comparable to that of Haslam *et al.*[32]. We note that although the values of the objective function and the %AAD of this work are slightly lower than those of Haslam *et al.*, the difference cannot be considered significant; both parameter sets result in overall %AAD < 1.

It is also of interest to follow from the work of Swaminathan and Visco[56], where the intermolecular parameters reported for propene (also known as refrigerant R1270) have a potential range $\lambda = 1.8172$, which is of interest here since it is larger than 1.8. We consider two models for this molecule, one in which the number of segments m is optimized and the other case where m is fixed to the value reported in the literature ($m = 1.0152$). In the case of free m the objective function is minimised over a grid in the $m - \lambda$ space, with the corresponding contour plot presenting a wide minimum area for a range of values of the parameter m, as for the n-alkanes. The minimum in the grid is identified at $m = 2.3$ and $\lambda = 1.70$ (with corresponding values of $\sigma = 3.2169$ Å and $\epsilon/k_B = 142.891$ K). The optimized parameters are presented in Table I together with the corresponding %AAD. We have also carried out optimizations with a fixed value of $m = 1.0152$ in order to compare the work of Swaminathan and Visco[56]. As before, fixing m leads to objective functions with less local minima. The minimum in the grid is identified at $\lambda = 1.25$ and $\sigma = 4.8$ Å (with corresponding value of $\epsilon/k_B = 480.566$ K). The optimal set of parameters found is presented in Table I. For comparison the molecular parameters for R1270 presented by Swaminathan and Visco[56] are given in Table I. We note that the low value of the square-well depth found in their model is related to the fact while that while in the article they state that propene is modelled without sites, in fact they modelled this compound including two association sites[57]. However, as can be seen from our fully optimized model (cf. table I), a very good representation of the phase behaviour of this system can be obtained without the need for association sites.

C. Small polar molecules

It is well-known that dipole-dipole interactions are very long-ranged, and that special techniques such as the Ewald sum are needed to simulate dipolar systems[58]. Recently considerable effort has also been placed to incorporate explicit polar terms into the SAFT framework[59]-[65]. In the original SAFT-VR approach, however, dipoles are treated in an effective way via a variable square-well range, so that given the long-ranged nature of the dipole-dipole interaction values of $\lambda > 1.8$ may at first be expected. Indeed, models for polar molecules have been presented where the upper bound of $\lambda = 1.8$ was used[39,49]. Here we consider three small polar molecules; carbon monoxide (CO) which is weakly polar (its dipole moment μ in the gas phase is reported as 0.12 Debye), hydrogen chloride (HCl, $\mu = 1.08$ Debye) and hydrogen Bromide ($\mu = 0.80$ HBr), and model them as non-associating molecules treating dipole-dipole interactions only in an effective way via the variable range of the attractive square-well. CO is modelled as non-spherical so that four intermolecular parameters (m, σ, ϵ and λ) need to be determined, while HCl and HBr are treated as spherical (i.e., $m = 1$). We follow the proceduce presented in section II studying the $m - \lambda$ or $\sigma - \lambda$ parameter spaces to identify the global minimum of the objective function given in equation (7). In the case of CO we carry out optimizations in the $m - \lambda$ space as well as in the $\sigma - \lambda$ space with $m = 1.519$ fixed for comparison with a model available in the literature[48]. The final optimal intermolecular model parameters, together with values for the AAD%, are presented in table I. As can be seen, contrary to what may be expected, we find values of the square-well potential that are within the range of the original SAFT-VR approach (i.e., $\lambda < 1.8$). It is in fact interesting to note that the optimal models for HCl and HBr present values of the square-well range shorter than those for non-polar molecules.

Since in the standard SAFT-VR approach dipoles are not incorporated explicitly, another approach to treat strongly polar compounds is by introducing associating sites. We have also followed this approach for HCl and HBr. A two-site model is used, where one site of type e models the electronegative atom and the other of type H the proton. The sites are placed at a distance $r_d/\sigma = 0.25$ from the centre of the spherical segment and have a range r_c/σ so that when two sites are closer than this distance an attractive interaction ϵ^{HB} is realised. We carry out a set of optimizations in a grid at discrete fixed values of λ and ϵ^{HB} described in section III. The optimized model parameters are presented in table II. We find

that using these models, the overall AAD% are lower than when no sites are included. This may indicate that the two-site models are better suited to treat polar molecules, but the fact that added parameters are needed to characterize the site-site interactions obscures this conclusion (the more parameters the better a model should be expected to perform).

D. Water

Although in recent work[33] an exhaustive study of water models and intermolecular parameters has been presented, it is useful for completeness to assess here the impact of implementing the extended SAFT-VR equation to model this compound. We have obtained the association energy ϵ^{HB}/k_B - potential range λ contour plot of the objective function and %AAD (Figure 8) for a fixed value of $m = 1$, since water is treated as spherical. In this case a wide region of minima is observed, with the minimum of the grid found for $\epsilon^{HB}/k_B = 1282$ K and $\lambda = 1.65$ (with corresponding $\sigma = 3.0353$ Å, $\epsilon/k_B = 347.7427$ K, and $r_c = 0.6804$),. A final optimization with the initial point and tight bounds leads to the parameter set presented in Table II. The set of parameters obtained here is entirely consistent with the one published earlier[33]; exact mathematical agreement cannot be expected due to the different mappings of the original SAFT-VR and the one used here. A key finding is that we confirm that even in the case of a strongly polar molecule, and even though dipolar interactions are not treated explicitly in the SAFT-VR approach, the square-well potential of the model is relatively short-ranged.

V. DISCUSSION AND CONCLUSIONS

The generalised SAFT-VR equation of state[42] has been used to model a number of compounds including simple non-polar molecules such as argon, chain-like molecules such as n-alkanes, polar molecules such as nitrogen, benzene and carbon dioxide, carbon monoxide, hydrogen chloride and hydrogen bromide, and hydrogen bonding molecules such as water as examples. We first of all confirm the accuracy of the approach in comparison with computer simulation data and with the calculations of Tan *et al.*[43]. In terms of comparisons with experimental phase behaviour, a relative least-square objective function of the sum of residuals of pressure and saturated liquid density as compared to experimental data is min-

imised at fixed grid points of two of the intermolecular parameters of the molecular model. This technique has been shown to be useful in identifying regions of minima in the complex objective function surface of multiparameter equations of state such as SAFT-VR[33].

A key aim of this paper was to evaluate the need to call on models with long square-well ranges ($\lambda > 1.8$). In the case of models for electrolytes, Tan *et al.*[43] have found it is necessary to use values for the potential range $\lambda > 1.8$, and in the treatment of critical states, McCabe and Kiselev[44,45] made use of the generalised SAFT-VR approach used here. We find however that, in terms of modelling the phase behaviour of non-electrolytes, when critical approaches are not implemented, there does not appear to be a need.

We find this result slightly disappointing, but entirely sensible. In fact, in the generalisation of the SAFT-VR equation it is shown how longer ranges of the square-well potential correspond to a phase behaviour closer to the mean-field limit of van der Waals, which is usually associated with dispersion interactions (as opposed to the longer-ranged non-conformal polar interactions). In this respect, it can be seen that even for polar compounds the range of the square-well may not be expected to be longer. It is also useful to recall that a Boltzmann averaging of the dipole-dipole interaction energy over all orientations leads to the Keesom potential[169], an interaction which varies as the sixth inverse power of intermolecular distance; i.e. comparable to the range of van der Waals or dispersion forces and which can be treated as contributing to the overall van der Waals intermolecular interaction.

Using propene as an example, we have shown that the few instances when optimal models previously obtained in the literature have resulted in values of the square-well potential range $\lambda > 1.8$, these were most likely due to optimization problems, understood in terms of local minima being identified as opposed to the global minimum. As discussed by Clark *et al.*[33], reducing the dimensionality of the optimization problem in multiparameter equations of state such as SAFT-type approaches, and using a global (if discrete) search of the remaining space, leads to an optimal model that is closest to the global minimum and not one of the local minima.

ACKNOWLEDGMENTS

M.C.dR. acknowledges the Programme Alβan from European Union Programme of High Level Scholarships for Latin America (identification number E03D21773VE) for a Fellowship.

Authors also acknowledge financial support from project number FIS2007-66079-C02-02 of the Spanish Dirección General de Investigación. Additional support from Universidad de Huelva and Junta de Andalucía is also acknowledged.

---

[1] W. R. Smith, D. Henderson, and R. D. Murphy. *J. Chem. Phys.*, **61**, 2911, 1974.

[2] D. Henderson, W. G. Madden, and D. Fitts. *J. Chem. Phys.*, **64**, 5026, 1976.

[3] W. R. Smith, D. Henderson, and Y. Tago. *J. Chem. Phys.*, **67**, 5308, 1977.

[4] J. A. Barker and D. J. Henderson. *J. Chem. Phys.*, **47**, 2856, 1967.

[5] D. J. Henderson, O. H. Scalise, and W. R. Smith. *J. Chem. Phys.*, **72**, 2341, 1980.

[6] P. Bolhuis and D. Frenkel. *Phys. Rev. Lett.*, **72**, 2211, 1994.

[7] J. R. Elliott and L. Hu. *J. Chem. Phys.*, **111**, 3043, 1999.

[8] J. Largo, J. R. Solana, S. B. Yuste, and A. Santos. *J. Chem. Phys.*, **122**, 084510, 2005.

[9] A. L. Benavides, L. A. del Pino, A. Gil-Villegas, and F. Sastre. *J. Chem. Phys.*, **125**, 204715, 2006.

[10] E. Zaccarelli, F. Sciortino and P. Tartaglia. *J. Phys. Cond. Matter*, **16**, 4849, 2004.

[11] E. Zaccarelli, S. V. Buldyrev, E. La Nave, A. J. Moreno, I. Saika-Voivod, F. Sciortino and P. Tartaglia. *Phys. Rev. Lett.*, **16**, 4849, 2004.

[12] F. del Río, E. Ávalos, R. Espíndola, L. F. Rull, G. Jackson, and S. Lago. *Mol. Phys.*, **100**, 2531, 2002.

[13] E. Schöll-Paschinger, A. L. Benavides, and R. Castañeda-Priego. *J. Chem. Phys.*, **123**, 234513, 2005.

[14] A. Gil-Villegas, F. del Rio, and A. L. Benavides. *Fluid Phase Equil.*, **119**, 97, 1996.

[15] A. L. Benavides and F. del Rio. *Mol. Phys.*, **68**, 983, 1989.

[16] M. S. Wertheim. *J. Stat. Phys.*, **35**, 19, 1984.

[17] M. S. Wertheim. *J. Stat. Phys.*, **35**, 35, 1984.

[18] M. S. Wertheim. *J. Stat. Phys.*, **42**, 459, 1986.

[19] M. S. Wertheim. *J. Stat. Phys.*, **42**, 477, 1986.

[20] M. S. Wertheim. *J. Chem. Phys.*, **85**, 2929, 1986.

[21] M. S. Wertheim. *J. Chem. Phys.*, **87**, 7323, 1987.

[22] W. G. Chapman, K. E. Gubbins, G. Jackson, and M. Radosz. *Fluid Phase Equil.*, **52**, 31, 1989.

[23] W. G. Chapman, K. E. Gubbins, G. Jackson, and M. Radosz. *Ind. Eng. Chem. Res.*, **29**, 1709, 1990.

[24] A. Gil-Villegas, A. Galindo, P. J. Whitehead, S. J. Mills, G. Jackson, and A. N. Burgess. *J. Chem. Phys.*, **106**, 4168, 1997.

[25] A. Galindo, L. A. Davies, A. Gil-Villegas, and G. Jackson. *Mol. Phys.*, **93**, 241, 1998.

[26] C. McCabe, A. Galindo, A. Gil-Villegas, and G. Jackson. *Int. J. Thermophys.*, **19**, 1511, 1998.

[27] A. Galindo, L. J. Florusse, and C. J. Peters. *Fluid Phase Equil.*, **158-160**, 123, 1999.

[28] P. Paricaud, A. Galindo, and G. Jackson. *Fluid Phase Equil.*, **194–197**, 87, 2002.

[29] B. H. Patel, P. Paricaud, A. Galindo, and G. C. Maitland. *Ind. Eng. Chem. Res.*, **42**, 3809, 2003.

[30] P. Paricaud, A. Galindo, and G. Jackson. *Ind. Eng. Chem. Res.*, **43**, 6871, 2004.

[31] A. Valtz, A. Chapoy, C. Coquelet, P. Paricaud, and D. Richon. *Fluid Phase Equil.*, **226**, 333, 2004.

[32] A. J. Haslam, N. von Solms, C. S. Adjiman, A. Galindo, G. Jackson, P. Paricaud, M. L. Michelsen, and G. M. Kontogeorgis. *Fluid Phase Equil.*, **243**, 74, 2006.

[33] G. N. I. Clark, A. J. Haslam, A. Galindo, and G. Jackson. *Mol. Phys.*, **104**, 3561, 2006.

[34] T. Lafitte, D. Bessieres, M. M. Pineiro, and J. L. Daridon. *J. Chem. Phys.*, **124**, 024509, 2006.

[35] T. Lafitte, M. M. Pineiro, J. Daridon, and D. Bessieres. *J. Phys. Chem. B*, **111**, 3447, 2007.

[36] J. A. Barker and D. J. Henderson. *J. Chem. Phys.*, **47**, 4714, 1967.

[37] J. A. Barker and D. J. Henderson. *Rev. Mod. Phys*, **48**, 587, 1976.

[38] N. F. Carnahan and K. E. Starling. *J. Chem. Phys.*, **51**, 635, 1969.

[39] A. Galindo, A. Gil-Villegas, G. Jackson, and A. N. Burgess. *J. Phys. Chem. B*, **103**, 10272, 1999.

[40] A. Galindo, S. J. Burton, G. Jackson, D. P. Visco, and D. A. Kofke. *Mol. Phys.*, **100**, 2241, 2002.

[41] A. Galindo, A. Gil-Villegas, P. J. Whitehead, G. Jackson, and A. N. Burgess. *J. Phys. Chem. B*, **102**, 7632, 1998.

[42] B. H. Patel, H. Docherty, S. Varga, A. Galindo, and G. C. Maitland. *Mol. Phys.*, **103**, 129, 2005.

[43] S. P. Tan, X. Ji, H. Adidharma, and M. Radosz. *J. Phys. Chem. B*, **110**, 16694, 2006.

[44] C. McCabe and S. B. Kiselev. *Fluid Phase Equil.*, **219**, 3, 2004.

[45] C. McCabe and S. B. Kiselev. *Ind. Eng. Chem. Res.*, **43**, 2839, 2004.

[46] G. V. Reklaitis, A. Ravindran, and K. M. Ragsdell. *Engineering Optimization: Methods and Applications*. John Wiley & Sons Inc, 2nd edition, 2004.

[47] U. Westhaus, T. Droge, and R. Sass. *Fluid Phase Equil.*, **158**, 429, 1999.

[48] T. J. Sheldon, B. Giner, C. S. Adjiman, A. Galindo, G. Jackson, D. Jaquemin, V. Wathelet, and E. A. Perpete. *The derivation on size parameters for the SAFT-VR equation of state from quantum mechanical calculations*, volume in "Multiscale modelling of polymer properties", ed. M. Laso and E. A. Perpete. Elsevier: Amsterdam, 2006.

[49] A. Galindo and F. J. Blas. *J. Phys. Chem. B*, **106**, 4503, 2002.

[50] F. J. Blas and A. Galindo. *Fluid Phase Equil.*, **194–197**, 501, 2002.

[51] M. C. dos Ramos, F. J. Blas and A. Galindo. *Fluid Phase Equil.*, **261**, 359, 2007.

[52] M. C. dos Ramos, F. J. Blas and A. Galindo. *J. Phys. Chem. C.*, **111**, 15924, 2007.

[53] M. L. McGlashan. *Pure Applied Chemistry*, **57**, 89, 1985.

[54] G. M. Schneider. *Pure Applied Chemistry*, **63**, 1313, 1991.

[55] J. S. Rowlinson and F. L. Swinton. *Liquids and Liquid Mixtures*, volume 3rd ed. Butterworth Scientific: London, 1982.

[56] S. Swaminathan and D. P. Visco. *Ind. Eng. Chem. Res.*, **44**, 4798, 2005.

[57] D. P. Visco, Privarte Communication.

[58] D. Frenkel and B. Smit, *Understanding Molecular Simulation*, 2nd ed, Academic Press: San Diego, USA, 2002.

[59] P. K. Jog and W. G. Chapman, *Mol. Phys.*, **97**, 307, 1999.

[60] Z. P. Liu, Y. G. Li and K. Y. Chan, *Ind. Eng. Chem. Res.*, **40**, 973, 2001.

[61] P. K. Jog, S. G. Sauer, J. Blaesing and W. G. Chapman, *Ind. Eng. Chem. Res.*, **40**, 4641, 2001.

[62] F. Tumakaka and G. Sadowski, *Fluid Phase Equil.*, **217**, 233, 2004.

[63] E. K. Karakatsani, T. Spyriouni and I. G. Economou, *AIChE J.*, **51**, 2328, 2005.

[64] J. Gross and J. Vrabec, *AIChE J.*, **52**, 1194, 2006.

[65] H. G. Zhao and C. McCabe, J. Chem. Phys., **125**, 104504, 2006.

[66] N. B. Vargaftik. *Dictionary of Thermophysical Properties of Gases and Liquids*. Moskva, 1972.

[67] J. C. G. Calado, F. A. Dias, J. N. C. Lopes, and L. P. N. Rebelo. *J. Phys. Chem. B*, **104**, 8735, 2000.

[68] A. M. Clark, F. Din, J. Robb, A. Michels, T. Wassenaar, and T. Zwittering. *Physica Amsterdam*, **17**, 876, 1951.

[69] J. C. G. Calado and W. B. Streett. *Fluid Phase Equil.*, **2**, 275, 1979.

[70] R. Gilgen, R. Kleinrahm, and W. Wagner. *J. Chem. Thermodynamics*, **26**, 399, 1994.

[71] O. Verbeke, V. Jansoone, R. Gielen, and J. de Boelpaep. *J. Phys. Chem.*, **73**, 4076, 1969.

[72] E. C. C. Baly and F. G. Donnan. *J. Chem. Soc.*, **81**, 907, 1902.

[73] W. B. Streett and L. A. K. Staveley. *J. Chem. Phys.*, **50**, 2302, 1969.

[74] W. Wagner. *Cryogenics*, **13**, 470, 1973.

[75] P. Nowak, R. Kleinrahm, and W. Wagner. *J. Chem. Thermodynamics*, **29**, 1157, 1997.

[76] J. H. Dymond and J. Robertson. *Int. J. Thermophys.*, **6**, 21, 1985.

[77] S. Malanowski and M. T. Raetzsch. *Fluid Phase Equil.*, **7**, 55, 1981.

[78] H. Kratzke, R. Niepmann, E. Spillner, and F. Kohler. *Fluid Phase Equil.*, **16**, 287, 1984.

[79] P. G. McCracken, T. S. Storvick, and J. M. Smith. *J. Chem. Eng. Data*, **5**, 130, 1960.

[80] J. M. Lenoir, K. E. Hayworth, and H. G. Hipkin. *J. Chem. Eng. Data*, **16**, 280, 1971.

[81] C. F. Jenkin and D. R. Pye. *Philos. Trans. R. Soc. London Ser. A*, **213**, 67, 1914.

[82] J. M. Sengers, H. Levelt, and W. T. Chen. *J. Chem. Phys.*, **56**, 595, 1972.

[83] C. H. Meyers and M. S. van Dusen. *J. Res. Nat. Bur. Std.*, **10**, 381, 1933.

[84] L. A. Webster and A. J. Kidnay. *J. Chem. Eng. Data*, **46**, 759, 2001.

[85] J. G. Harris and K. H. Yung. *J. Phys. Chem.*, **99**, 12021, 1995.

[86] P. Nowak, T. Tielkes, R. Kleinrahm, and W. Wagner. *J. Chem. Thermodynamics*, **29**, 885, 1997.

[87] *Design Institute for Physical Property Data*, American Institute of Chemical Engineers, 1987.

[88] L. Djordjevich and R. A. Budenholzer. *J. Chem. Eng. Data*, **15**, 10, 1970.

[89] G. F. Carruth and R. Kobayashi. *J. Chem. Eng. Data*, **18**, 115, 1973.

[90] J. Regnier. *J. Chim. Phys. Phys. Chim. Biol.*, **69**, 942, 1972.

[91] D. R. Douslin and R. H. Harrison. *J. Chem. Thermodynamics*, **5**, 491, 1973.

[92] A. K. Pal, G. P. Pope, Y. Arai, N. F. Carnahan, and R. Kobayashi. *J. Chem. Eng. Data*, **21**, 394, 1976.

[93] L. J. Florusse and C. J. Peters. *Fluid Phase Equil.*, **202**, 1, 2002.

[94] M. B. King and R. S. Mahmud. *Fluid Phase Equil.*, **27**, 309, 1986.

[95] S. Hendl, J. Millat, E. Vogel, V. Vesovic, W. A. Wakeham, J. Luettmer-Strathmann, J. V.

Sengers, and M. J. Assael. *Int. J. Thermophys.*, **15**, 1, 1994.

[96] L. A. Bulavin, P. G. Ivanitsky, A. N. Maistrenko, Y. B. Melnichenko, and Y. I. Shimansky. *Ukr. Fys. Zh.*, **27**, 1042, 1982.

[97] H. Lu, D. M. Newitt, and M. Ruhemann. *Proc. R. Soc. London, Ser. A*, **178**, 506, 1941.

[98] W. M. Haynes and M. J. Hiza. *J. Chem. Thermodynamics*, **9**, 179, 1977.

[99] S. K. Talitskikh and P. G. Khalatur. *Zh. Fiz. Khim.*, **66**, 137, 1992.

[100] C. McCabe and G. Jackson. *Phys. Chem. Chem. Phys.*, **1**, 2057, 1999.

[101] W. B. Kay. *J. Chem. Eng. Data*, **15**, 46, 1970.

[102] R. H. P. Thomas and R. H. Harrison. *J. Chem. Eng. Data*, **27**, 1, 1982.

[103] V. G. Niesen and J. C. Rainwater. *J. Chem. Thermodynamics*, **22**, 777, 1990.

[104] H. Kratzke and S. Mueller. *J. Chem. Thermodynamics*, **16**, 1157, 1984.

[105] J. D. Kemp and C. J. Egan. *J. Am. Chem. Soc.*, **60**, 1521, 1938.

[106] I. M. Abdulagatov, L. N. Levina, Z. R. Zakaryaev, and O. N. Mamchenkova. *Zh. Prikl. Khim.*, **69**, 1655, 1996.

[107] J. F. Ely and R. Kobayashi. *J. Chem. Eng. Data*, **23**, 221, 1978.

[108] R. C. Wackher, C. B. Linn, and A. V. Grosse. *Ind. Eng. Chem.*, **37**, 464, 1945.

[109] B. H. Sage, D. C. Webster, and W. N. Lacey. *Ind. Eng. Chem.*, **29**, 1188, 1937.

[110] W. B. Kay. *Ind. Eng. Chem.*, **32**, 358, 1940.

[111] T. W. Legatski. *Ind. Eng. Chem.*, **34**, 1240, 1942.

[112] M. R. Lipkin, J. A. Davison, and S. S. Kurtz. *Ind. Eng. Chem.*, **34**, 976, 1942.

[113] R. H. Olds, H. H. Reamer, B. H. Sage, and W. N. Lacey. *Ind. Eng. Chem.*, **36**, 282, 1944.

[114] T. R. Das, C. O. Reed, and P. T. Eubank. *J. Chem. Eng. Data*, **18**, 244, 1973.

[115] J. L. Flebbe, D. A. Barclay, and D. B. Manley. *J. Chem. Eng. Data*, **27**, 405, 1982.

[116] W. Warowny. *J. Chem. Eng. Data*, **41**, 689, 1996.

[117] C. R. McClune. *Cryogenics*, **16**, 289, 1976.

[118] O. Sifner and F. Nemec. *Chem. Prum.*, **36**, 420, 1986.

[119] J. H. Mcmicking and W. B. Kay. *Proc. Amer. Petrol. Inst. Sec. 3*, **45**, 75, 1965.

[120] S. Young. *J. Chem. Soc. Trans.*, **77**, 1145, 1900.

[121] J. H. Dymond and K. J. Young. *Int. J. Thermophys.*, **1**, 331, 1980.

[122] A. G. Badaljian, A. S. Keramidi, D. S. Kurumov, and B. A. Grigoryev. *Izv. Vyssh. Uchebn. Zaved. Neft Gaz*, **29**, 54, 1986.

[123] C. B. Willingham, W. J. Taylor, J. M. Pignocco, and F. D. Rossini. *J. Res. Nat. Bur. Std.*, **35**, 219, 1945.

[124] G. A. Burrell and I. W. Robertson. *J. Am. Chem. Soc.*, **37**, 2188, 1915.

[125] F. M. Seibert and G. A. Burrell. *J. Am. Chem. Soc.*, **37**, 2683, 1915.

[126] O. Maass and C. H. Wright. *J. Am. Chem. Soc.*, **43**, 1098, 1921.

[127] C. A. Winkler and O. Maass. *Can. J. Res. Sect. B*, **9**, 610, 1933.

[128] F. R. Morehouse and O. Maass. *Can. J. Res. Sect. B*, **11**, 637, 1934.

[129] T. M. Powell and W. F. Giauque. *J. Am. Chem. Soc.*, **61**, 2366, 1939.

[130] W. E. Vaughan and N. R. Graves. *Ind. Eng. Chem.*, **32**, 1252, 1940.

[131] A. B. Lamb and E. E. Roper. *J. Am. Chem. Soc.*, **62**, 806, 1940.

[132] Densities of liquefied petroleum. Technical Committee, Gases Natural Gasoline Association of America. *Ind. Eng. Chem.*, 1942.

[133] P. S. Farrington and B. H. Sage. *Ind. Eng. Chem.*, **41**, 1734, 1949.

[134] G. H. Goff, P. S. Farrington, and B. H. Sage. *Ind. Eng. Chem.*, **42**, 735, 1950.

[135] L. N. Canjar, M. Goldman, and H. Marchman. *Ind. Eng. Chem.*, **43**, 1186, 1951.

[136] R. A. McKay, A. H. Reamer, B. H. Sage, and W. N. Lacey. *Ind. Eng. Chem.*, **43**, 2112, 1951.

[137] H. H. Reamer and B. H. Sage. *Ind. Eng. Chem.*, **43**, 1628, 1951.

[138] A. W. Tickner and F. P. Lossing. *J. Phys. Colloid Chem.*, **55**, 733, 1951.

[139] A. W. Francis. *J. Phys. Chem.*, **58**, 1099, 1954.

[140] D. W. Morecroft. *J. Inst. Pet. London*, **44**, 433, 1958.

[141] M. Hirata, T. Hakuta, and T. Onoda. *Int. Chem. Eng.*, **8**, 175, 1968.

[142] H. Enokido, T. Shinoda, and Y. Mashiko. *Bull. Chem. Soc. Jpn.*, **42**, 3415, 1969.

[143] D. B. Manley and G. W. Swift. *J. Chem. Eng. Data*, **16**, 301, 1971.

[144] D. R. Laurance and G. W. Swift. *J. Chem. Eng. Data*, **17**, 333, 1972.

[145] L. Grauso, A. Fredenslund, and J. Mollerup. *Fluid Phase Equil.*, **1**, 13, 1977.

[146] H. K. Bae, K. Nagahama, and M. Hirata. *J. Chem. Eng. Japan*, **14**, 1, 1981.

[147] K. Noda, M. Sakai, and K. Ishida. *J. Chem. Eng. Data*, **27**, 32, 1982.

[148] W. R. Parrish and D. M. Sltton. *J. Chem. Eng. Data*, **27**, 303, 1982.

[149] A. Harmens. *J. Chem. Eng. Data*, **30**, 230, 1985.

[150] K. Ohgaki, M. Kageyama, and T. Katayama. *J. Chem. Eng. Japan*, **23**, 763, 1990.

[151] K. Ohgaki, S. Umezono, and T. Katayama. *J. Supercrit. Fluids*, **3**, 78, 1990.

[152] K. Noda, K. Inoue, T. Asai, and K. Ishida. *J. Chem. Eng. Data*, **38**, 9, 1993.

[153] M. Kleiber. *Fluid Phase Equil.*, **92**, 149, 1994.

[154] N. F. Giles, H. L. Wilson, and W. V. Wilding. *J. Chem. Eng. Data*, **41**, 1223, 1996.

[155] H. P. Gros, M. S. Zabaloy, and E. A. Brignole. *J. Chem. Eng. Data*, **41**, 335, 1996.

[156] A. J. Apelblat and E. Manzurola. *J. Chem. Thermodynamics*, **31**, 869, 1999.

[157] F. G. Keyes. *J. Mech. Eng. Sci.*, **53**, 132, 1931.

[158] I. M. Abdulagatov, V. I. Dvoryanchikov, and A. N. Kamalov. *J. Chem. Thermodynamics*, **29**, 1387, 1997.

[159] I. M. Abdulagatov, V. I. Dvoryanchikov, and A. N. Kamalov. *J. Chem. Eng. Data*, **43**, 830, 1998.

[160] W. J. Gildseth, F. H. Spedding, and A. Habensh. *J. Chem. Eng. Data*, **17**, 402, 1972.

[161] N. S. Osborne. *J. Res. Nat. Bur. Std.*, **10**, 155, 1933.

[162] D. R. Douslin and A. Osborn. *J. Sci. Instrum.*, **42**, 369, 1965.

[163] A. Egerton. *Philos. Trans. R. Soc. London Ser. A*, **231**, 147, 1932.

[164] L. Besley and G. A. Bottomle. *J. Chem. Thermodynamics*, **5**, 397, 1973.

[165] L. Verlet and J. J. Weis. *Physical Review A*, **5**, 939, 1972.

[166] J. P. Hansen and I. R. McDonald. *Theory of simple liquids*, volume 2nd ed. Academic Press: London, 1990.

[167] L. Vega, E. de Miguel, L. F. Rull, G. Jackson, and I. A. McLure. *J. Chem. Phys.*, **96**, 2296, 1992.

[168] G. Orkoulas and A. Z. Panagiotopoulos. *J. Chem. Phys.*, **110**, 1581, 1999.

[169] J. Israelachvili. *Intermolecular and surface forces*, 2nd ed. Academic Press: London, 1991.

Table I: Optimised intermolecular parameters for non-associating real substances for the generalised SAFT-VR for longer potential ranges.

	m	λ	σ (Å)	ϵ/k_B (K)	$f_{\text{objective}}$	%AAD	N_{exp}
Ar	1.0000 [b]	1.47225	3.30219	127.380	0.17960	1.3508	221[66–73]
C_2H_6	2.0966 [a]	1.75984	3.07979	110.750	0.12970	2.4435	135[88–99]
	1.3333 [b]	1.41429	3.81131	253.022	0.33710	3.8605	135[88–99]
	1.3333 [c,100]	1.44900	3.78800	241.800	0.66250	6.0653	
C_3H_8	2.4162 [a]	1.69285	3.25909	143.285	0.18160	2.8668	135[66,88,89,98,101–107]
	1.6667 [b]	1.44687	3.87357	266.610	0.29223	2.9684	135[66,88,89,98,101–107]
	1.6667 [c,100]	1.45200	3.87300	261.900	0.24050	2.6904	
n-C_4H_{10}	2.3843 [a]	1.60509	3.57315	198.487	0.18400	2.5352	77[66,89,98,101,108–118]
	2.0000 [b]	1.49857	3.87565	261.829	0.19385	2.2954	77[66,89,98,101,108–118]
	2.0000 [c,100]	1.50100	3.88700	253.600	0.24650	2.8861	
n-C_8H_{18}	4.3968 [a]	1.75917	3.45352	154.753	0.03920	1.4492	137[66,88,119–123]
	3.3333 [b]	1.54815	3.94697	267.204	0.11211	2.0617	137[66,88,119–123]
	3.3333 [c,100]	1.57400	3.94500	250.300	0.28610	3.9227	
C_6H_6	2.7521 [a]	1.71922	3.35218	197.775	0.00653	0.5596	97[66,76–80]
	2.7604 [c,48]	1.73910	3.34730	193.620	0.00751	0.6019	
CO_2	3.0274 [a]	1.75849	2.29391	94.865	0.00304	0.4092	50[81–86]
	2.0000 [b]	1.52676	2.77393	179.317	0.00395	0.5396	50[81–86]
	2.0000 [c,49]	1.51570	2.78640	179.270	0.00497	0.6838	
N_2	1.4110 [a]	1.56717	3.05750	78.346	0.00549	0.5055	98[66,74,75]
	1.3000 [b]	1.51652	3.17571	88.605	0.00625	0.5053	98[66,74,75]
	1.3000 [c,32]	1.53400	3.19400	84.530	0.01703	0.8360	
R1270	2.3182 [a]	1.68104	3.22085	147.165	0.52605	2.6327	283[97,118,124–155]
	1.0152 [b]	1.27235	4.70262	458.300	1.23795	5.1456	283[97,118,124–155]
	1.0152 [c,56]	1.81720	4.41230	142.219	$\gg 10$	$\gg 10$	
CO	1.6275 [a]	1.63095	2.90812	68.776	0.00829	0.6386	152[87]
	1.5190 [b]	1.57850	2.99908	78.139	0.00945	0.6200	152[87]
	1.5190 [c,48]	1.60040	3.00420	73.950	0.00786	0.5995	
HCl	1.0000 [b]	1.3311	3.6190	365.235	0.25167	3.4960	91[87]
HBr	1.0000 [b]	1.3448	3.8210	386.655	0.06075	1.4996	90[87]

[a] Corresponds to the results when the adjustment is done for all molecular parameters. [b] Corresponds to results when m is fixed and then the adjustment is done for the rest of the molecular parameters. [c] Corresponds to results obtained with the optimization procedure using the original SAFT-VR approach and the parameters are those found in the reference given.

Table II: Optimised intermolecular parameters for associating real substances for the generalised SAFT-VR for longer potential ranges.

	m	λ	σ (Å)	ϵ/k_B (K)	ϵ^{HB}/k_B (K)	r_c	$f_{\text{objective}}$	$\%AAD$	N_{exp}
H_2O	1.0 [b]	1.65921	3.03528	342.371	1279.405	0.68044	0.03840	0.5958	583[156–164]
	1.0 [c,33]	1.71825	3.03300	300.433	1336.951	0.68433	0.03786	0.5960	
HCl	1.0 [b]	1.50245	3.46735	261.505	673.8676	0.65313	0.03167	1.1246	91[87]
HBr	1.0 [b]	1.46592	3.72646	279.924	608.2353	0.74888	0.00097	0.2175	90[87]

[b] and [c] same as Table I.

LIST OF FIGURES

Figure 1. Models for (a) non-associating compounds used in this work: argon, nitrogen, carbon dioxide, carbon monoxide, benzene, *n*-alkanes (ethane, propane, *n*-butane and *n*-octane) and R1270; model for water (b) and model for hydrogen chloride and hydrogen bromide (c), the associating systems studied, together with the square-well potential (part (d)).

Figure 2. The first perturbation term (A_1/NkT) as a function of the packing fraction (η) for square-well fluids of different ranges. Solid lines are obtained using the Padé expression for the effective packing fraction presented in a previous work[42] while dashed lines are obtained using the expression for the effective packing fraction presented by Tan *et al.*[43]. Squares correspond to the numerical solution of the equation (2), where the radial distribution function was treated in the Perkus-Yevick approximation with the Verlet-Weis modification[165,166].

Figure 3. Vapour-liquid coexistence for the square-well fluid of range (a) 1.25, (b) 1.50, (c) 1.75, (d) 2.00, (e) 2.30 and (f) 2.50. Solid lines are obtained using the Padé expression for the effective packing fraction presented in a previous work[42] while dashed lines are obtained using the expression for the effective packing fraction presented by Tan *et al.*[43]. Symbols correspond to simulation data: Diamonds are the GEMC data of Vega *et al.*[167], circles are the hybrid MC data of del Rio *et al.*[12], triangles are the MD data of Elliot and Hu[7] and crosses are the NVT data of Patel *et al.*[42].

Figure 4. Clausius-Clapeyron representation of the vapour pressure for square-well fluids of different ranges. Solid lines are obtained using the Padé expression for the effective packing fraction presented in a previous work[42] while dashed lines are obtained using the expression for the effective packing fraction presented by Tan *et al.*[43]. Symbols correspond to simulation data: Diamonds are the GEMC data of Vega *et al.*[167], circles are the hybrid MC data of del Rio *et al.*[12], triangles are the MD data of Elliot and Hu[7], crosses are the NVT data of Patel *et al.*[42], and pluses are the data of Orkoulas and Panagiotopoulos[168].

Figure 5. Representation of the objective function (parts (a) and (c)) and %AAD values (parts (b) and (d)) obtained when the intermolecular parameters (m, ϵ/k_B, σ and λ) of the extended SAFT-VR approach are adjusted to the experimental data of vapour pressure and saturated liquid density of *n-butane* (C_4H_{10})[66,89,98,101,108–118]. Part (a) and (b) show the

results for the optimization procedure when m and λ are fixed values for each grid point, i.e. ϵ/k_B and σ are adjusted; and part (c) and (d) show the results for the optimization procedure when σ and λ are fixed values for each grid point and also fixing $m = 2.0$, i.e. only ϵ/k_B is adjusted.

Figure 6. Representation of the objective function (a) and %AAD values (b) obtained when the intermolecular parameters (m, ϵ/k_B, σ and λ) of the extended SAFT-VR approach are adjusted to the experimental data of vapour pressure and saturated liquid density of *benzene* (C_6H_6)[66,76–80] Part (a) and (b) show the results for the optimization procedure when m and λ are fixed values for each grid point, i.e. ϵ/k_B and σ are adjusted.

Figure 7. Representation of the objective function (parts (a) and (c)) and %AAD values (parts (b) and (c)) obtained when the intermolecular parameters (m, ϵ/k_B, σ and λ) of the extended SAFT-VR approach are adjusted to the experimental data of vapour pressure and saturated liquid density of *carbon dioxide* (CO_2)[81–86]. Part (a) and (b) show the results for the optimization procedure when m and λ are fixed values for each grid point, i.e. ϵ/k_B and σ are adjusted; and part (c) and (d) show the results for the optimization procedure when σ and λ are fixed values for each grid point and also fixing $m = 2.0$, i.e. only ϵ/k_B is adjusted.

Figure 8. Representation of the objective function (a) and %AAD values (b) obtained when the intermolecular parameters (σ, ϵ/k_B, λ, ϵ^{HB}/k_B and r_c) of the extended SAFT-VR approach are adjusted to the experimental data of vapour pressure and saturated liquid density of *water* (H_2O)[156–164]. These results represent the optimization procedure when ϵ^{HB}/k_B and λ are fixed values for each grid point and also fixing $m = 1.0$, i.e. σ, ϵ/k_B and r_c are adjusted.

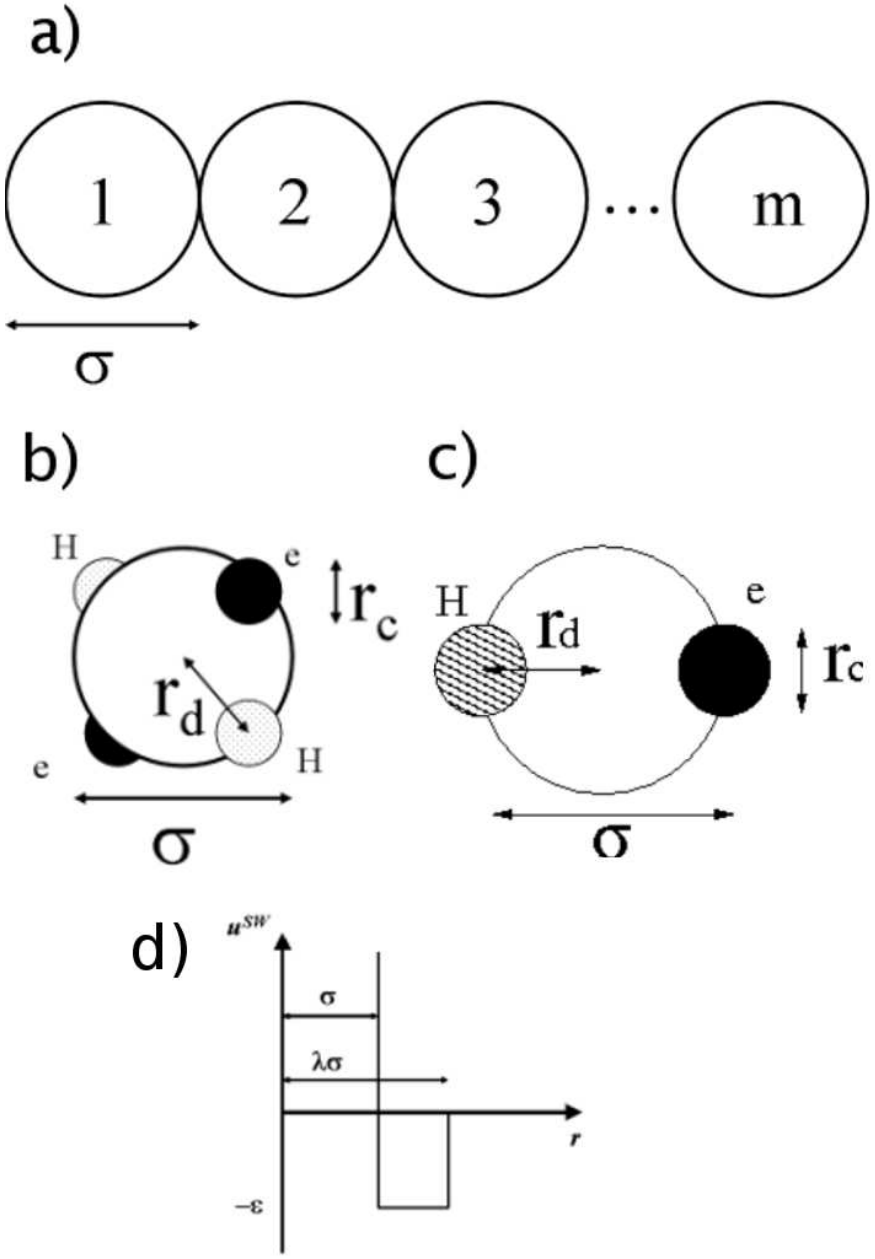

FIG. 1: dos Ramos, Galindo, Docherty and Blas

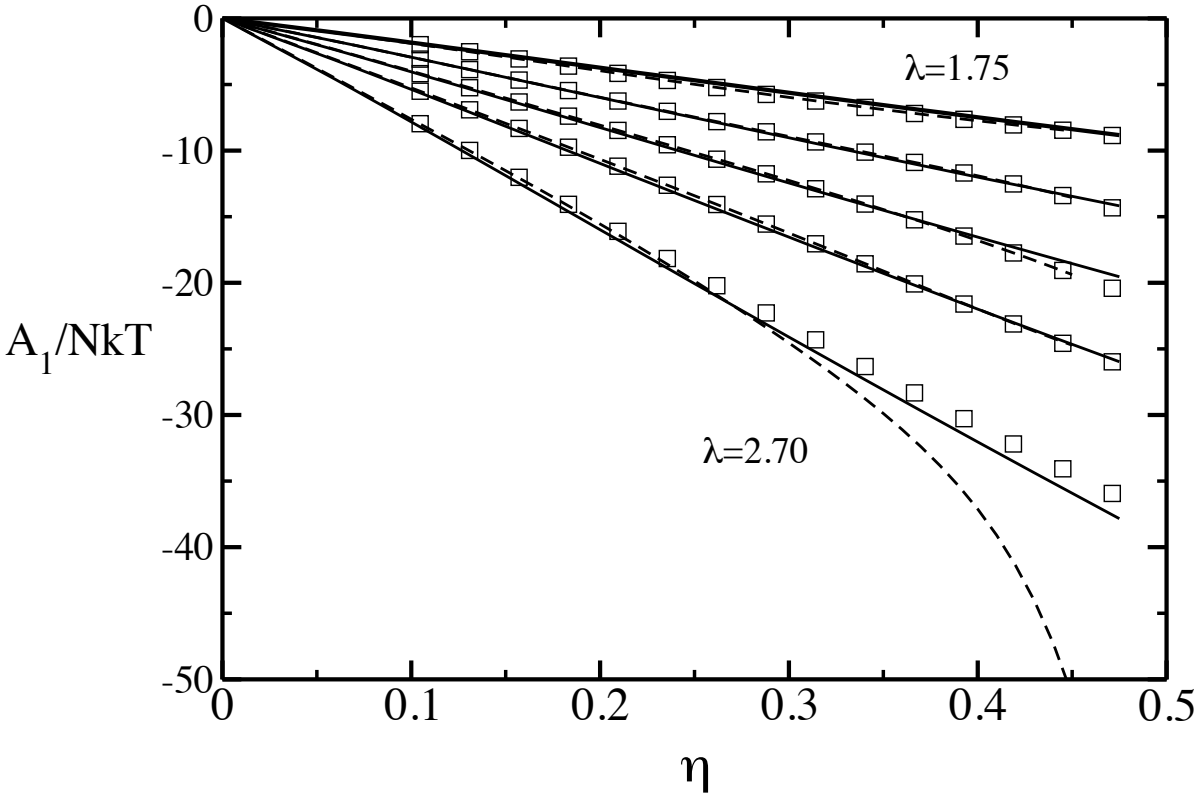

FIG. 2: dos Ramos, Galindo, Docherty and Blas

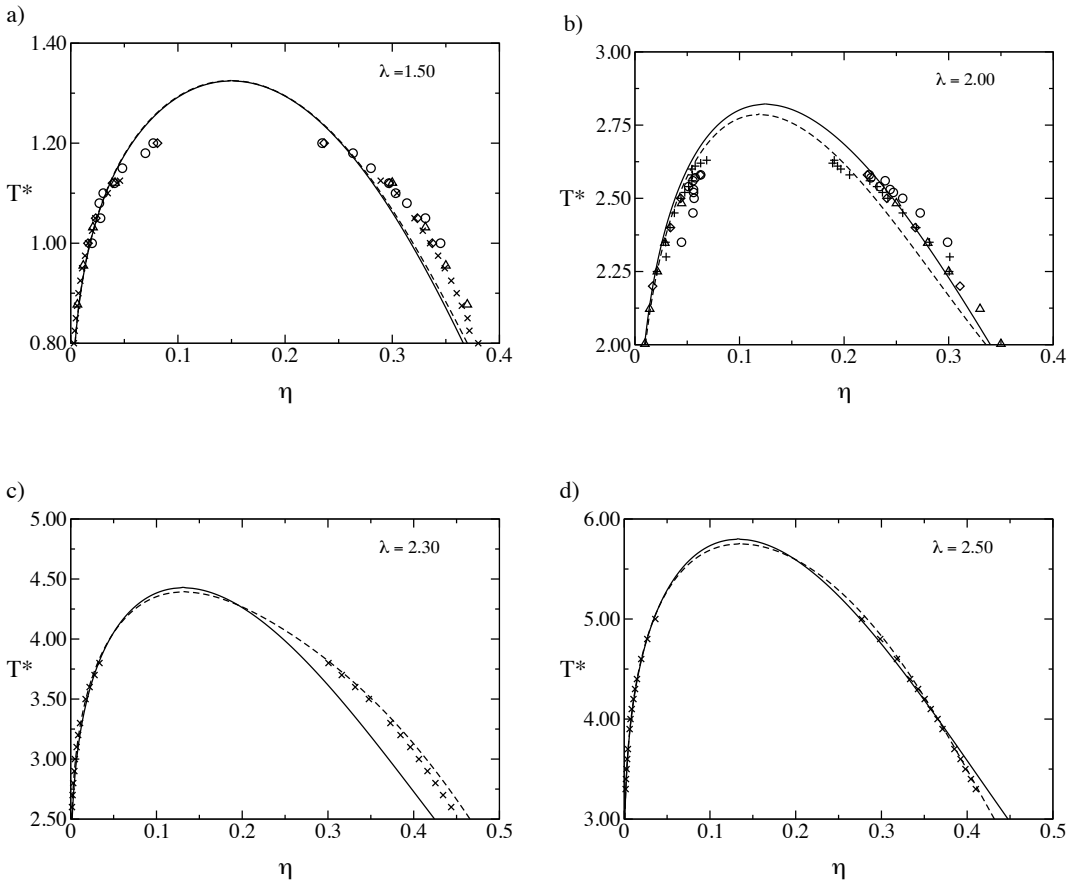

FIG. 3: dos Ramos, Galindo, Docherty and Blas

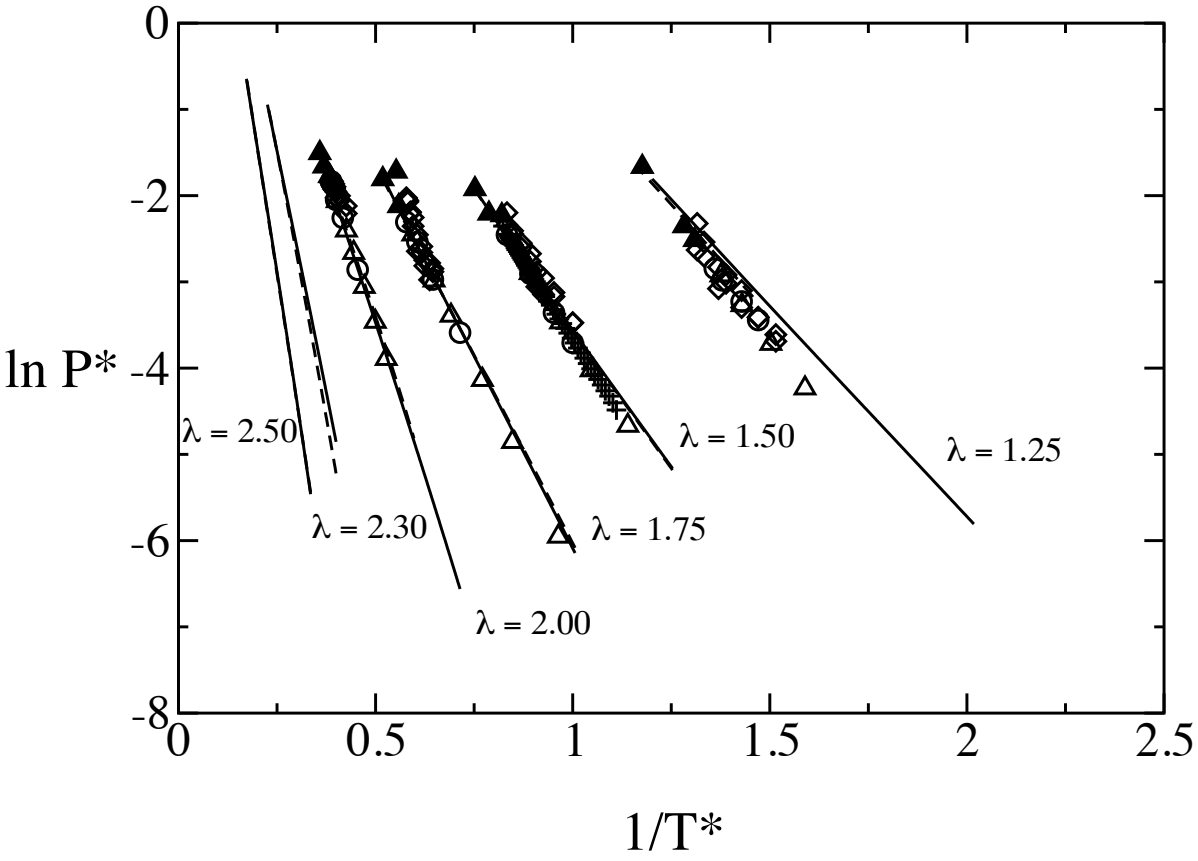

FIG. 4: dos Ramos, Galindo, Docherty and Blas

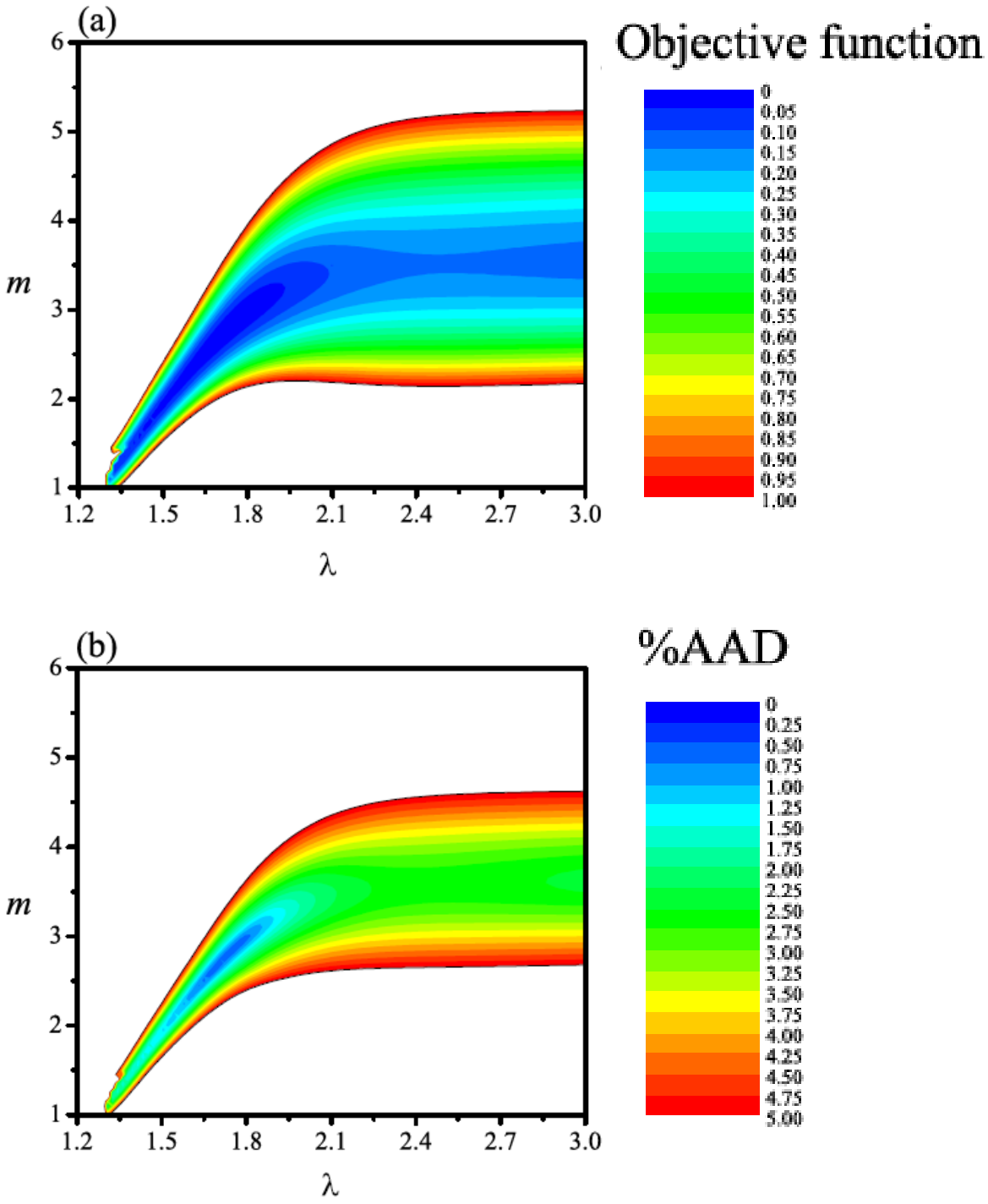

Figure 5: dos Ramos et al.

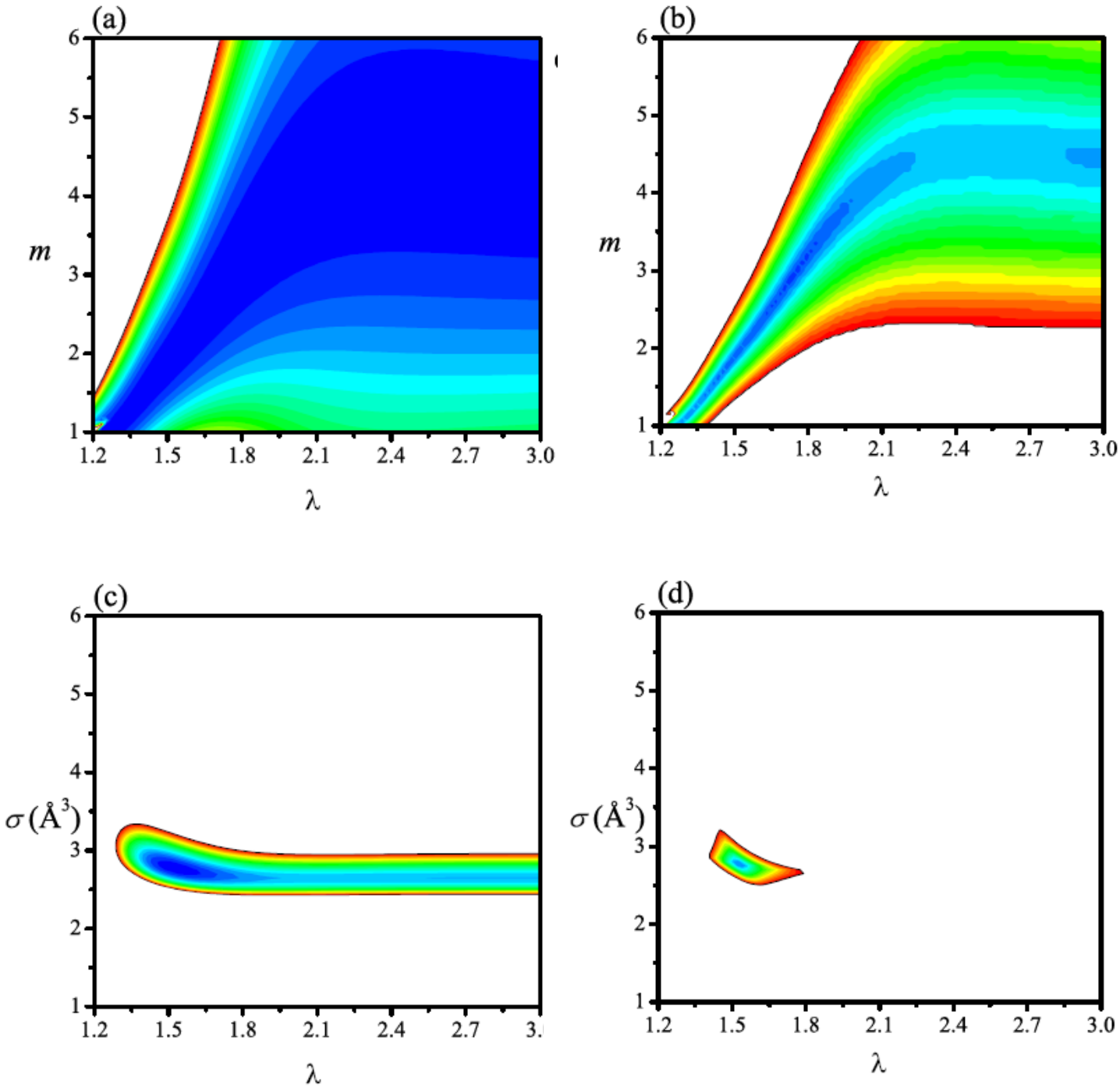

Figure 6: dos Ramos et al.

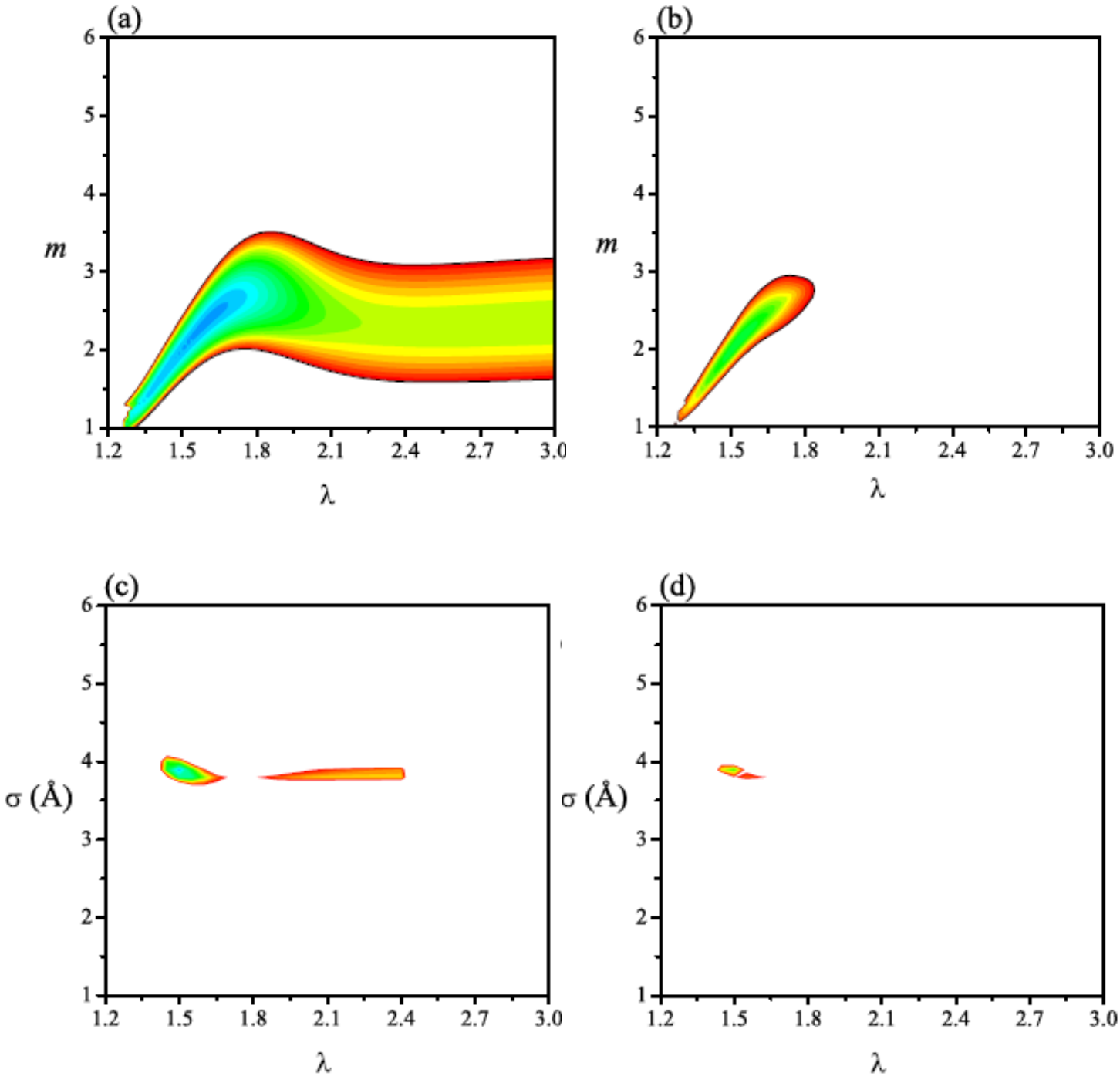

Figure 7: dos Ramos et al.

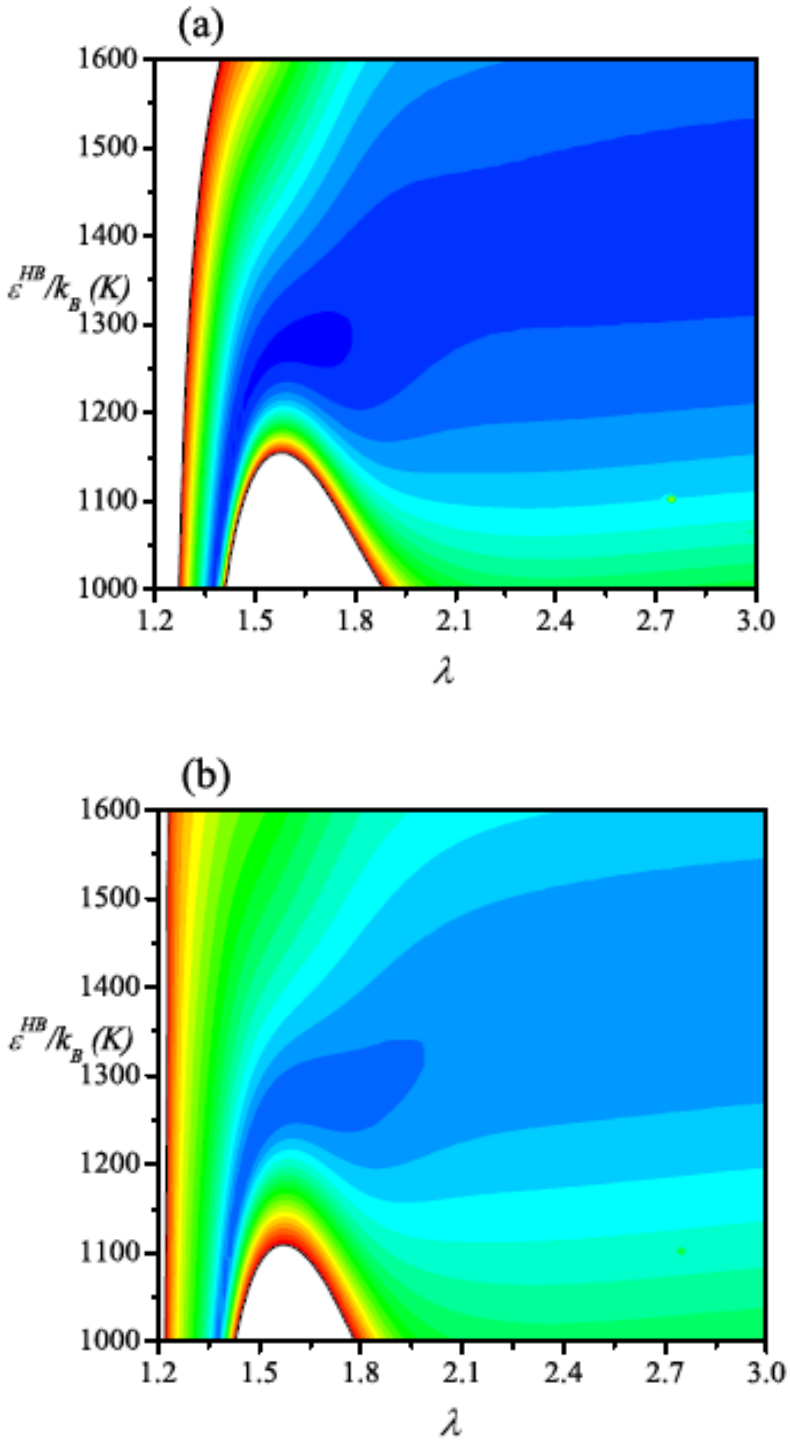

Figure 8: dos Ramos et al.